Smart Structures and Systems, *Vol. 14, No. 5 (2014) 917-942*
DOI: http://dx.doi.org/10.12989/sss.2014.14.5.917

An integrated approach for structural health monitoring using an in-house built fiber optic system and non-parametric data analysis

Masoud Malekzadeh[1a], Mustafa Gul[2b], Il-Bum Kwon[3c] and Necati Catbas[*1]

[1]*Department of Civil, Environmental, and Construction Engineering, University of Central Florida, 4000 Central Florida Blvd, Orlando, Florida, United States*
[2]*Department of Civil and Environmental Engineering, University of Alberta, 9105 116th St, Edmonton, Alberta, Canada*
[3]*Center for Safety Measurements, Korea Research Institute of Standards and Science, 1 Doryonga-dong, Yuseong-gu, Daejeon, 305-340, South Korea*

(Received July 8, 2013, Revised February 20, 2014, Accepted February 26, 2014)

Abstract. Multivariate statistics based damage detection algorithms employed in conjunction with novel sensing technologies are attracting more attention for long term Structural Health Monitoring of civil infrastructure. In this study, two practical data driven methods are investigated utilizing strain data captured from a 4-span bridge model by Fiber Bragg Grating (FBG) sensors as part of a bridge health monitoring study. The most common and critical bridge damage scenarios were simulated on the representative bridge model equipped with FBG sensors. A high speed FBG interrogator system is developed by the authors to collect the strain responses under moving vehicle loads using FBG sensors. Two data driven methods, Moving Principal Component Analysis (MPCA) and Moving Cross Correlation Analysis (MCCA), are coded and implemented to handle and process the large amount of data. The efficiency of the SHM system with FBG sensors, MPCA and MCCA methods for detecting and localizing damage is explored with several experiments. Based on the findings presented in this paper, the MPCA and MCCA coupled with FBG sensors can be deemed to deliver promising results to detect both local and global damage implemented on the bridge structure.

Keywords: structural health monitoring; fiber optic sensor; non-parametric damage detection algorithm; principal component analysis; cross correlation analysis

1. Introduction

As a result of advances in sensing and information technologies, Structural Health Monitoring (SHM) is rapidly developing as a multi-disciplinary technology solution for condition assessment and performance evaluation of civil infrastructure systems, particularly bridges (Aktan and Catbas

*Corresponding author, Professor, E-mail: catbas@ucf.edu
[a] Ph.D. Candidate, E-mail: m.malekzadeh@knights.ucf.edu
[b] Assistant Professor, E-mail: mustafa.gul@ualberta.ca
[c] Ph.D. Principal Research Scientist, E-mail: ibkwon@kriss.re.kr

http://www.techno-press.org/?journal=sss&subpage=8 ISSN: 1738-1584 (Print), 1738-1991 (Online)

2000, Chang 1999, Balageas 2006, Farrar and Worden 2007, Catbas and Kijewski-Correa 2013). Several studies report that about a quarter of the bridges are either structurally deficient or functionally obsolete in the United States (Puentes 2008). Accordingly, $20.5 billion annual investment is required to substantially enhance current bridge conditions (ASCE 2013).

As a consequence, there is an unavoidable and continuously increasing demand for monitoring the behavior of existing structures over time (Glisic *et al*. 2010). SHM can be considered as a promising technology for effective and efficient management of different structures such as bridges, buildings, and airplanes (Brownjohn *et al*. 2004, Sohn *et al*. 2003, Glisic *et al*. 2010). Bridges are critical components of the transportation network and also considered as critical and strategic life-line structures. Accordingly, bridges have always received a significant amount of attention in terms of condition evaluation and assessment by utilizing SHM technologies. As a result, a number of investigations have been designed and implemented to demonstrate SHM of bridge structures (Brownjohn *et al*. 1995, Aktan *et al*. 1996, Enright and Frangopol 1999, Cardini and DeWolf 2009, Catbas *et al*. 2010, Catbas *et al*. 2012).

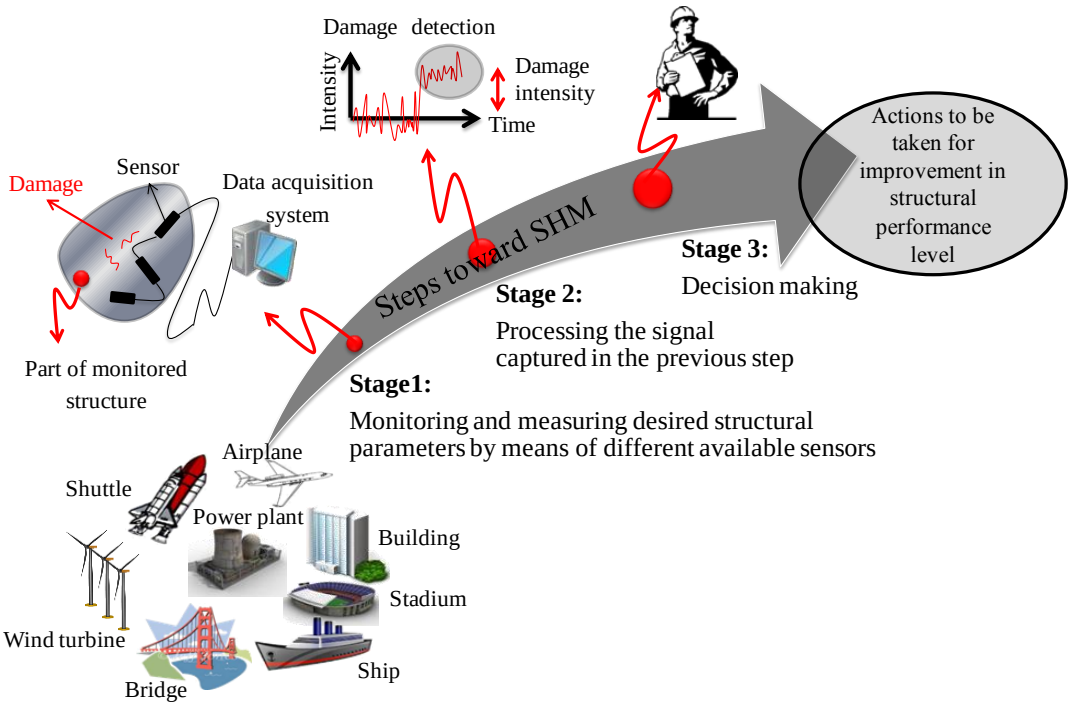

Fig. 1 Individual stages involved in SHM process

Main stages for SHM implementation are briefly summarized and illustrated in Fig. 1. It is fairly clear that the first two basic stages of SHM are critical phases in order to accomplish the predefined SHM objectives for decision making. The first stage, referred as collection and processing, highly relies on having a properly designed and well-distributed network of sensors. In other words, the major goal of the first stage is to equip a structure with sensors that would provide

useful data about the condition and performance of the structure in order to make engineering and management decisions such as bridge closure, condition-based maintenance, strengthening, limiting traffic etc. The selection of sensors that are appropriate for the measurement objectives satisfying the measurement type, resolution, range, ruggedness is important. Optical sensors and in particular Fiber Bragg Grating (FBG) sensors are well suited alternatives to the traditional sensors in terms of several aspects, such as spatial resolution, durability, stability and immunity to electrical noise (Morey *et al*. 1989, Ferdinand *et al*. 1997, Yin *et al*. 2008, Richard *et al*. 2012). Consequently, FBG sensors hold a great deal of potential for civil structural health monitoring (Vohra *et al*. 1999, Todd *et al*. 1999, Todd *et al*. 2000, Johnson 1999, Inaudi 2002, Ansari 2005, Glisic and Inausi 2008).

With a properly designed instrumentation plan and carefully selected sensors for measuring desired structural parameters at the critical areas along the monitored structure, it is possible to generate data for extracting the useful information as illustrated in the signal processing stage of Fig. 1. In this second stage, there are basically two approaches to analyze data for detecting changes and damage. These two approaches can be categorized as non-parametric and parametric methods (Worden 1997). Non-parametric methods are also known as model-free, data-driven, non-physics based or direct signal analysis methods. Similarly, the parametric methods are also called model-based, structural or physics-based methods. The methodologies using these approaches follow specific procedures and they are applicable in distinct contexts. A method will be preferred over another one based on desired SHM objectives. If the objective is to provide a better physical conceptualization or developing a prediction model, then parametric approaches may be better alternatives while dependency on behaviour model is the main downside associated with this type of algorithms.

Alternatively non-parametric approaches can be better alternatives in the circumstances in which creating a behavioural model is either time consuming or expensive (Omenzetter *et al*. 2004,Nicoud *et al*. 2005, Lanata 2005, Worden and Barton 2004, Laory 2011, Catbas *et al*. 2012, Malekzadeh *et al*. 2012, Malekzadeh *et al*. 2013). In fact, non-parametric approaches are free of geometrical and material information as utilization and interpretation of structural models are not needed. The use scenarios, advantages and disadvantages of these approaches are summarized in Table 1. In an ideal SHM implementation, these two approaches could be utilized in a complementary manner.

1.1 Objective and scope of the paper

For a successful SHM implementation, change and/or damage detection algorithms are critical to provide useful information effectively and efficiently. Numerous damage detection methods have been developed and implemented in the context of SHM. The authors have been conducting research for sensing and data analysis in the laboratory and also in the field. In this particular study, two algorithms, which can be referred as Moving Principal Component Analysis (MPCA) and Moving Cross Correlation Analysis (MCCA), are investigated using FBG sensors on a specially designed 4-span highway bridge model in the laboratory.

This unique four span bridge model is phenomenologically representative of common highway bridges in terms of its static and dynamic response as well as its structural components and characteristics such as the deck, girders, composite action, boundary conditions etc (Kwon *et al*. 2011). A number of damage conditions are simulated on the bridge model based on the feedback from bridge engineers from four different States' Departments of Transportation. SHM data

generated under operating traffic loading on the bridge model are analyzed to evaluate the efficiency of both MPCA and MCCA for the purpose of bridge monitoring implementations. In order to explore the development of low-cost fiber optic interrogator, use of FBGs and promising practical non-parametric methods in a comparative fashion for commonly experienced bridge problems, the authors carried out this research in an integrated manner towards a holistic SHM implementation on highway bridges. This paper includes a brief discussion about the basic principles of FBG sensing and the in-house developed FBG interrogator. Afterwards, the MPCA and MCCA techniques are discussed as non-parametric algorithms for damage/change identification. The experiments conducted on a 4-span bridge model structure, where global and local different damage scenarios are implemented, are presented, followed by the results from non-parametric methods for the illustration of damage detection ability. The paper concludes with discussions on sensitivity of these damage algorithms and workability of FBG sensors for bridge monitoring applications.

Table 1 A Comparison of Non-Parametric and Parametric Methods for Change/Damage Identification (Catbas *et al*. 2013)

Data Analysis Approaches	Scenarios for Common Use	Advantages	Disadvantages
Non-parametric Methods also known as • Data-Driven Methods; • Direct Signal Analysis; • Model-free Methods • Non-Physics-Based Methods	• Structure may not be a critical structure • Structural prediction is not critical • Many structures need to be monitored • There is time for training the system	• No need for models, therefore no modeling costs • May detect and localize changes/damage • Many options for signal analysis • Incremental training can track damage accumulation • Good for long-term use on structures for early detection of situations requiring model-based interpretation	• Physical interpretation of the signal may be difficult • Weak support for decisions on rehabilitation and repair • Indirect guidance for structural management activities such as inspection and further measurement • Cannot be used to justify replacement avoidance
Parametric Methods also known as • Structural Methods; • Model-based Methods; • Physics-Based Methods	• Design model is not accurate • Structure has strategic importance • Damage is suspected • There are structural management challenges	• Interpretation is easy when links between measurements and potential causes are explicit • The effects of changes in loading and use can be predicted • Guidance for further inspection and measurement • Consequences of future damage can be estimated • Support for planning rehabilitation and repair • May help justify replacement avoidance	• Modeling is expensive and time consuming • Errors in models and in measurements can lead to identification of the wrong model • Large numbers of candidate models are hard to manage • Identification of the right model could require several interpretation - measurement cycles • Complex structures with many elements have combinatorial challenges

2. Fiber Optic Sensor (FOS)

The sensor technology has been dominated by electrical sensors for decades. However, there are several features in which conventional sensors need significant improvements including sensitivity to electrical noise, heavy cabling labor etc. Due to these short comings, significant amount of effort has been devoted by researchers worldwide to the improvement of traditional sensors. Hence, these efforts resulted in a new generation of different sensors including optical fiber technology. The most superior aspects of FOS, in comparison to electrical-based sensors, are due to switching from electricity and copper wire to light and optical fiber, respectively. Eventually, these benefits turn the FOS into one of the most, if not the most, attractive sensors in SHM applications in terms of spatial resolution, durability, stability and immunity to electrical noise. There has been a dramatic increase in the FOS implementations in the context of SHM due to aforementioned advantages brought by these types of sensors. FBG sensors, which are point types of sensors, are among the widely used FOS. The basic working principles of FOS and FBG sensors are reflection and filtration of different wavelengths of light (Hill *et al*. 1978, Meltz *et al*. 1991). Beside the FBG sensors, Brillouin Optical Time Domain Analysis (BOTDA) and Brillouin Optical Time Domain Reflectometry (BOTDR) two of the widely used distributed types of FOS (Kwon *et al*. 2002, Kwon *et al*. 2011, Malekzadeh and Catbas 2012). For FBG sensors, grating property enables the optical fiber to transmit the entire wavelength except the particular reflected wavelength entitled as light grating resonance process. A brief introduction to theory of the optical fiber sensing with special emphasis on FBGs, which are employed in this study, is presented in the following sections. The basic working principle of FOS and FBG sensors is reflection and filtration of different wavelengths of light (Morey *et al*. 1989).

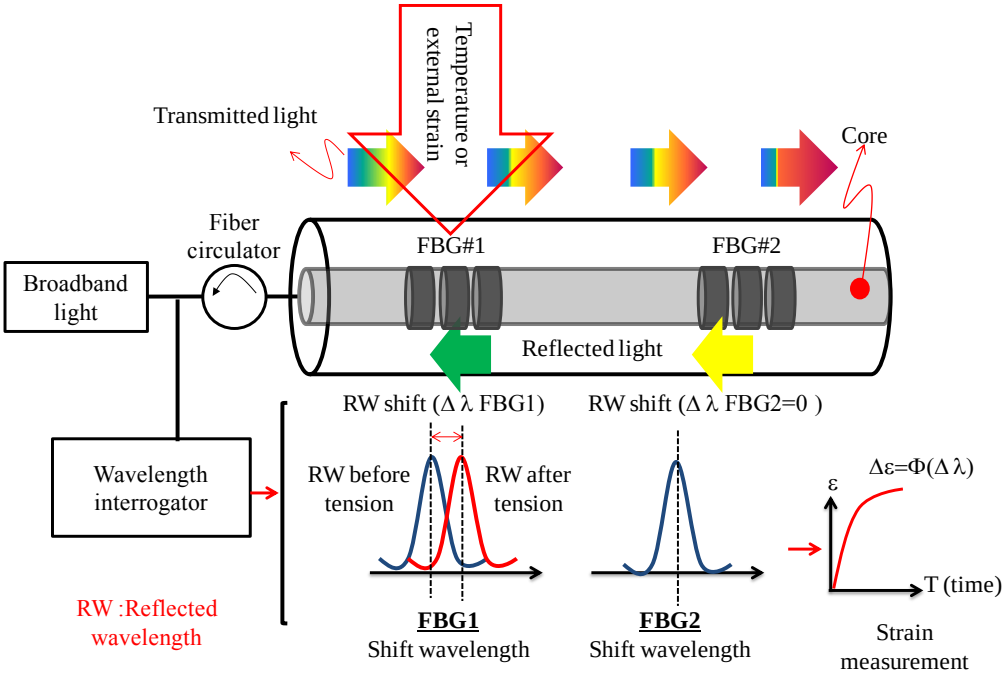

Fig. 2 Measurement principal of Fiber Bragg Grating (FBG) sensor

FBG system consists of an article interrogator launching infrared light into the core of an optical fiber. As white color, broadband light, travels down the fiber, it passes through grating segments, also identified as FBG, which is a series of article filter. These grating segments can filter certain wavelength or color while letting others pass through. This happens by periodically altering refractive index of fiber dictating the wavelengths that can pass and that will get reflected. External factors such as heat and vibration will cause a shift in wavelength of the reflected light. These variations can then translate into physical engineering units such as temperature and strain. The principal sensing technology of FBG is illustrated in Fig. 2.

2.1 FBG system developed In-house for SHM

As discussed above, Fiber Bragg grating (FBG) is a type of Bragg reflector that indexes in an optical fiber, which reflects particular, the Bragg wavelengths of light and transmits all others. A conventional FBG sensor system is composed of a broadband light source, FBGs, a wavelength interrogator, and system software, as shown in Fig. 2. When the broadband light is launched into an FBG, the reflection occurs at the FBG. Some light, of which wavelength satisfies Bragg condition of Eq. (1), is reflected, and the others pass the grating.

$$\lambda_B = 2n_e\Lambda \tag{1}$$

Where λ_B is the Bragg wavelength, n_e is the effective refractive index, and Λ is the grating period. When strain is induced in an FBG, the Bragg wavelength is expected to have a proportional shift. The strain can be easily determined by analyzing the change of the wavelength. According to this principle, FBG sensors can sense the grating period change due to strain variation, and they can measure strain without the influence from noise and light intensity perturbation. The wavelength shift is proportional to strain, and absolute strain can be measured by Eq. (2).

$$\frac{\Delta\lambda_B}{\lambda_B} = \{1 - \frac{n_e^2}{2}[p_{12} - \nu(p_{11} + p_{12})]\}\varepsilon \tag{2}$$

where p_{ij} are the silica photo-elastic tensor components, ε is the strain and ν is the Poisson's ratio.

The authors have designed and implemented an FBG sensor system for bridge monitoring. This cost-effective in house system is presented in the following and also Fig. 3. This system has three major elements: the power source, which needs to have a voltage about 5V and 0.4-0.5A to insure the optical light source is working properly; a minilite light source (ASE source), which has a wavelength range of 800-1650 nm, spectral width of 100 nm, output power up to 30 mW and it is operating temperature between 10-70 Celsius.

Finally, the most important part, the FBG interrogator has a wavelength range of 1525-1565 nm, while the resolution is about 1 pm. The operating frequency of the system is around 5 kHz and interface with USB. It requires the operating temperature between 0-70 Celsius. The last component is the circulator, which ensures that the reflected light is going back to the FBG interrogator and the interrogator is going to send the data directly to the computer to conduct the analysis (Fig. 3). After the design and manufacturing of this system, the measurements obtained using this system were verified against other conventional measurement system. The calibration

and verification studies on this FOS system are beyond the scope of this paper, and only data obtained for monitoring studies will be reported herein.

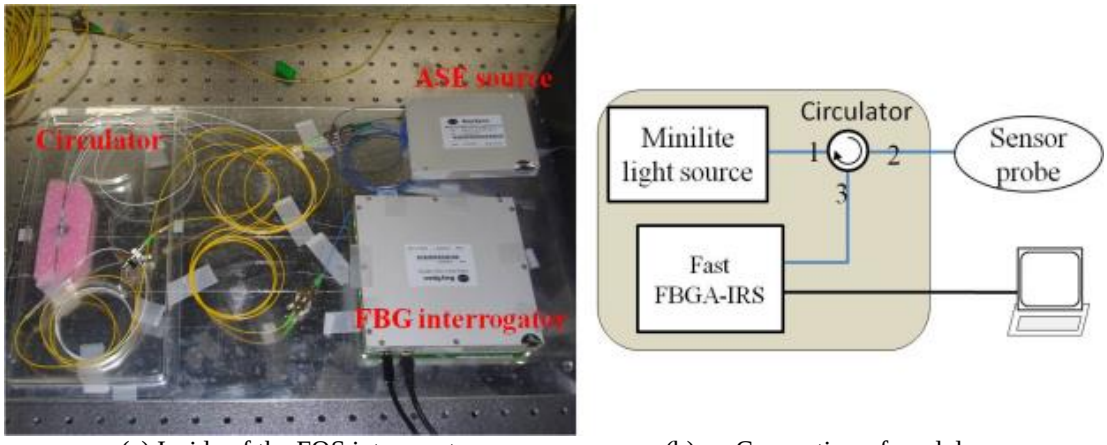

(a) Inside of the FOS interrogator (b) Connection of modules

Fig. 3 FBG interrogator (UCF in-house developed FBG system)

3. Model- free approach for data interpretation

3.1 Principal Component Analysis (PCA)

Long term monitoring of real life, large and complex structures requires dealing with multi-modal large datasets captured from different type of sensors. Therefore, efficient data analysis methods should be employed to deal with large sets of data and to evaluate the condition of the monitored structure by means of detecting any change that can be attributed to damage or change in operational conditions. In many cases, high dimensional parametric data analysis methods may not only be complicated but also time consuming. In addition, the interpretation of the results may be challenging.

In contrast, multivariate dimensionality reduction techniques are desirable methods for SHM to avoid such disadvantages. Principal Component Analysis (PCA) is one the most powerful techniques for reducing a complex data set to fewer dimensions. PCA is used for feature extraction from high dimensional data to reveal the most informative underlining patterns in fewer dimensions (Mujica *et al*. 2010). PCA can be referred as a projection/transformation method to turn a set of observations of possibly correlated variables, variable space, into sets of independent variables termed as principal components, principal space. The schematic presentation of this projection is demonstrated in Fig. 4. In fact, PCA can be considered as a projection technique in which the observations are projected from a high dimensional space named as original space (Fig. 4) into a less dimensional space so called principal component space.

This projection should be performed in such a way that the new coordinates would be laid in the directions in which the original data has the most variance so that this transformation does not end up with losing important information. In order to achieve this goal, the optimized plain in

original space should be identified in a way that projection of observations can be performed with the minimum possible residual value and consequently minimum possible loss of information; these procedures are illustrated in Fig. 4. The steps towards PCA analysis are explained in more details in the following sections.

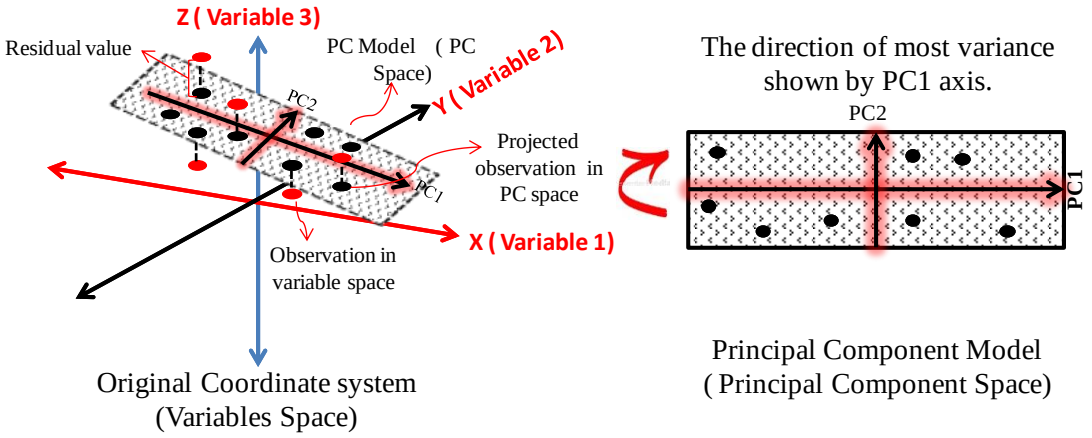

Fig. 4 Schematic demonstration of Principal Component Analysis

3.1.1 Constructing and scaling sensor network measurement data for PCA

The preliminary step for PCA is generating a main matrix by inserting time history of each variable (sensor) as illustrated in the following matrix

$$\begin{pmatrix} M_{t_{1^1}} & \cdots & M_{t_{1^n}} \\ \vdots & \ddots & \vdots \\ M_{t_{m^1}} & \cdots & M_{t_{m^n}} \end{pmatrix} \tag{3}$$

where the number of rows indicates the number of observations while the number of columns specifies the number of measured variables (sensors). In other words, $M_{t_{m^n}}$ represents the n^{th} observation collected at time t_m. There are different desired structural data that are collected through the SHM procedure including, strain, acceleration, displacement data etc. However, each of these parameters or measured variables has it own scale and magnitudes and as a result should be scaled before applying PCA or any other multivariate techniques. So as to solve this issue, several methods are recommended in the literature for scaling experimental data. The mots popular technique among all others, which is also implemented in this study, is autoscaling. Each variable (column) should be scaled in such a way that the distribution follows the standard Gaussian distribution. The following procedures have to be taken for performing the autoscale method.

$$\mu_{t_{ij}} = \frac{1}{m}\sum_{t_i=t_0}^{t_i=t_{end}} M_{t_{ij}} \tag{4}$$

$$\sigma^2{}_{t_{ij}} = \frac{1}{m-1}\sum_{t_i=t_0}^{t_i=t_{end}} (M_{t_{ij}} - \mu_{t_{ij}})^2 \tag{5}$$

Where $\mu_{t_{ij}}$ and $\sigma^2{}_{t_{ij}}$ are mean and variance respectively, corresponding to variable j (sensor j).

It should be also noted that *m* is the number of rows, which represent the number of observations. Therefore, the scaled variables are derived from the succeeding equation.

$$\overline{M}_{t_{ij}} = \frac{M_{t_{ij}} - \mu_{t_{ij}}}{\sigma^2{}_{t_{ij}}} \tag{6}$$

3.1.2 Covariance matrix and extraction of eigenvector and eigenvalues

Having a scaled data matrix, as it was discussed in details throughout previous sections, the covariance matrix is derived based on the following equation

$$C_M = \frac{1}{m-1} \bar{M}^T \bar{M} \tag{7}$$

where $\bar{M}$ denotes the scaled matrix achieved in section 3.1.1. The principal components of the original matrix can be found by extracting the eigenvectors and eigenvalues of the scaled matrix, which should satisfy the Eq. (8)

$$(C_M - \lambda_i)\psi_i = 0 \Longrightarrow i = 1, \dots, n \tag{8}$$

where ψ_i and λ_i are referred as eigenvectors and eigenvalues of the scaled matrix. *I* also denotes *n*x*n* identity matrix. In fact, the eigenvectors are laid in the directions in which the original data has the most variances. Typically, the first few components contain the most of the variance, and the rest is just corresponded to noise measurements. Due to this fact, in most cases, the first few principal components are only taken into account.

3.2 Moving Principal Component Analysis (MPCA)

Real life employment of SHM involves dealing with large amount of multivariate data. Only a small portion of abnormal data, in comparison to overall data, is available at the time when damage occurs. For detecting the changes in data sets effectively, the classical PCA should be improved to make it more practical for long term SHM data analysis. By means of PCA, the damage can be detectable only when the principal components (eigenvectors) are influenced by abnormal behavior. Subsequently, eigenvectors are subjected to change only if certain amount of abnormal data are captured and possibly affected the overall structure of data. This feature makes PCA less effective for long term SHM implementation. Moving principal component analysis (MPCA) was proposed by (Posenato *et al*. 2008) to address this challenge. Basically, MPCA computes the PCA within moving windows with a constant size. MPCA procedures applied in this study can be summarized in five different steps, which are presented here. Moreover, Fig. 5 gives details of MPCA algorithm designed for long term SHM applications.

Step 1: A data matrix should be generated by sorting the time history data from each sensor, or variable, into individual columns. Once the matrix is created, it should be divided into two segments, called training and monitoring phases. The training phase is intended for developing a baseline, confidence interval, based on normal condition, while monitoring phase is set for long term monitoring. The fixed moving windows should be well-defined. In fact, determining the window size precisely is one of the most critical issues in MPCA. The reader is referred to the paper by Posenato *et al*. (2008) for detailed information on selecting window size.

Step 2: PCA should be conducted for each window individually and results should be stored. Score matrix and coefficient matrix for each window should be calculated. The size of score

matrix is identical to the moving window whereas the number of rows for coefficient matrix is equal to number of sensors and the number of columns is identical to the number of principal components. The score matrix is representative of projected observations in the new coordinate system known as principal component coordinate and as a result the number of rows, observations, is equal to the amount of observations inside the fixed moving window. Alternatively, the coefficient matrix presents individual variables in terms of principal components. This step should be repeated for each window.

Step 3: A sensitive damage index should be selected in this step based on PCA outputs. The damage index (D_{si}) chosen for this study is square root of the sum of the squares of the first two principal components as shown in Eq. (9).

$$D_{S_i}=\sqrt{(PC_1)^2{}_i + (PC_2)^2{}_i} \tag{9}$$

Where $(PC_1)_i$ and $(PC_2)_i$ are the first and the second principal components of sensor i respectively. The reason to just incorporate the first two principal components in the damage index is that the most useful information in the data is covered by the first few principal components values. In fact, the first principal component corresponds to the direction of in which the projected data has the most variance while the second one is perpendicular to the first component. In other words, since more than 95% of the variance (calculated based on the preliminary study) is covered by the first two principal components, these two components are only incorporated in the damage index. It should be mentioned that the number of principal components, which should be considered depends on the data and there is not any prescription for all cases. However in the most cases the most variance is covered by the first two or three components. Therefore, the assumption is that, if any damage occurred in structure then it should affect the data and consequently variance of data and should be detected by this damage index. It should be mentioned that D_{si} are calculated for each windows along the time and consequently these values are plotted against time as shown in Fig. 5 and Step 3. As a final point, the confidence interval developed in the training phase should be considered as a benchmark (baseline) for detecting any possible damage sing the rest of the data.

3.3 Cross Correlation Analysis (CCA) and Moving CCA (MCCA)

The Cross Correlation Analysis (CCA) was recently proposed by the authors as a robust damage detection method using strain data for identifying and locating real damage on an existing movable bridge in Florida (Catbas *et al*. 2012) and the methodology is based on comparing the correlation matrices for the baseline and damaged cases. The cross correlation coefficients of the strain data at one location and all other locations are calculated to create the first row of the cross-correlation matrix. Then, the same procedure is repeated for all of the sensors and a full cross-correlation coefficient matrix is created. After obtaining cross correlation matrix, similar matrices are obtained subsequently for detecting and locating change by taking the difference of these matrices and baseline. The highest change in the difference matrix is related to change/damage and its location.

When comparing two signal pairs, the correlation can be obtained using Eq. (10)

$$\rho_{ij}(t) = \frac{\sum_{k=1}^{n}(S_i(t_k)-\mu_i)(S_j(t_k)-\mu_j)}{\sqrt{\sum_{k=1}^{n}(S_i(t_k)-\mu_i)^2}\sqrt{\sum_{k}^{n}(S_j(t_k)-\mu_j)^2}} \tag{10}$$

where ρ_{ij} is the correlation between the sensors *i* and *j*, n is the total number of time observations during the monitoring duration, $S_i(t_k)$ and $S_j(t_k)$ are the values from the sensors *i* and *j* at time t_k, and, μ_i, μ_j are the mean values of the data from the sensors *i* and *j*. Although the CCA showed promising results but it is not appropriate for long term monitoring of real life structure. For that reason, CCA algorithm should be improved in such a way that it can be practically applicable for real life condition assessment. In the following section basic theoretical background of MCCA algorithm, which is improved version of CCA is presented.

In order to make CCA method more practical and feasible for long-term monitoring, windowing technique is employed. As a result, Moving Cross Correlation Analysis (MCCA) was proposed as a promising upgraded version of CCA adapted for long term SHM (Puentes 2008). Determining a fixed size moving window, explained in MPCA section, that move along the time is a common aspect of MPCA and MCCA. The same matrix of data structure is developed and CCA is conducted for each individual window. Therefore, performing CCA for each moving window, correlation coefficient value is computed as correlation of sensor *i* and *j*. For detecting any possible abnormal behavior, the matrix of data is separated unequally into two segments as training and monitoring segments. The baseline behavior for each pair of sensors, sensors *i* and *j*, are defined by the confidence interval developed based on correlation coefficients obtained in the training phase. In the following step, the generated confidence intervals in training phase are considered as damage criteria for each pair of sensor throughout the monitoring phase. In other words, if the observed correlation coefficients for a given sensor *I* and *j* in monitoring phase exceed the confidence interval for the same sensors in training phase, it can be claimed that possible abnormal behavior is in progress in the structure.

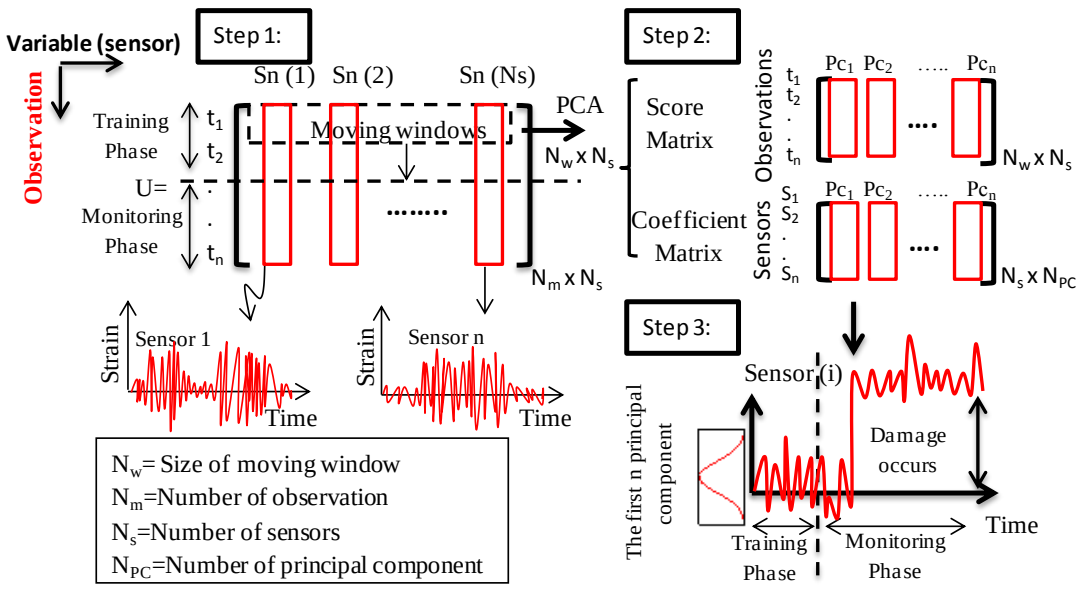

Fig. 5 Procedures for long term SHM using MPCA

4. Experimental study

4.1 Test structure

For the evaluation of both MPCA and MCCA algorithms using FBG sensors, several experiments with a laboratory bridge model (UCF 4-span Bridge Model) were designed and conducted taking of five common damage scenarios into consideration. The structure consists of two 120 cm approach (end) spans and two 304.8 cm main spans with a 3.18 mm thick, 121.92 cm wide steel deck supported by two HSS 25x25x3 girders separated 60.96 cm from each other. Using the 4-span bridge model in the UCF Structures Laboratory (Fig. 6), it is feasible to simulate and test a variety of damage scenarios that are commonly observed in bridge type structures (Zaurin and Catbas 2010).

It is possible to simulate most of the common boundary conditions, including roller, pin and fixed support. In addition to these, the bolts connecting the girders and deck can be loosened or removed at different locations to modify the stiffness of the system and to simulate damage. In other words, the first feature provides the opportunity to simulate the global damage scenarios, while the second one is desirable for local damage simulations. It should be pointed out that even though the structure is not a scaled down model of a specific bridge, its responses are representative of typical values for medium-span bridges. Radio controlled vehicles (15.7 kg) were crawled over the deck of the 4-span bridge to simulate traffic data on the bridge structure as seen in Fig. 7.

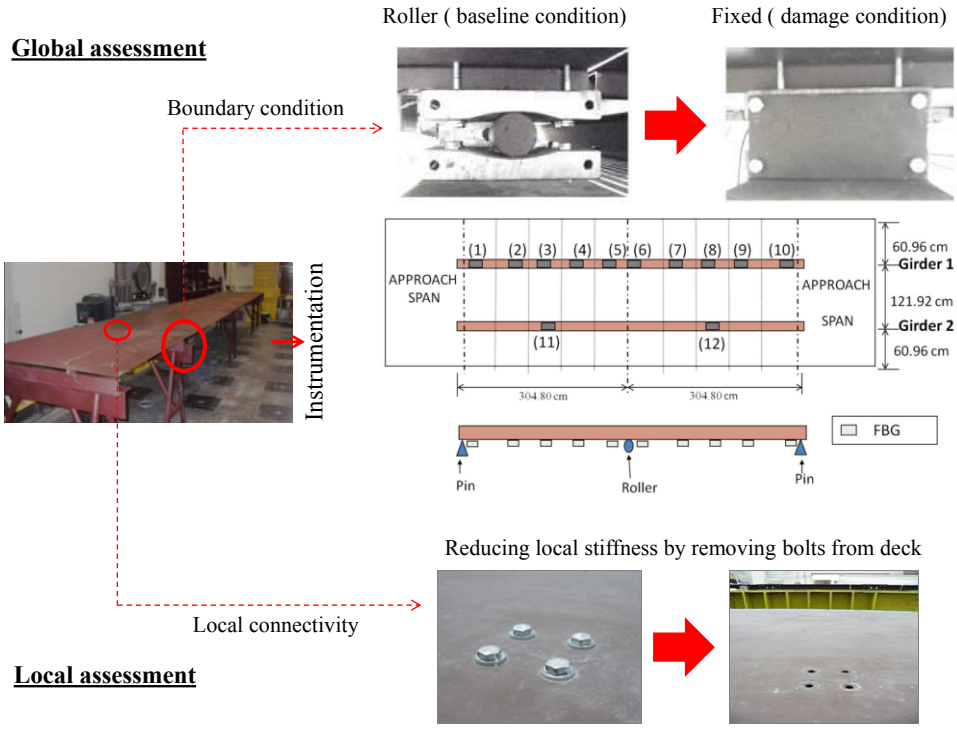

Fig. 6 Structural description and applied damage (UCF 4-span Bridge)

4.2 Damage scenarios

Based on the discussions with the Department of Transportation (DOT) engineers, several critical and common damage scenarios were identified and simulated on the 4-span bridge model. A crucial type of damage observed in bridges is unintended changes in boundary conditions. These types of changes may cause stress redistributions and in most cases it may result in additional load for different elements. Therefore, three cases were devoted to this type of damage using the advantage of the ability to shift from pinned to fix or roller condition or vice versa. Missing bolts and section stiffness reductions are also observed in existing bridges. Fourth and fifth damage cases simulate the loss of connectivity between the girder and the deck generating localized stiffness reduction. The damage scenarios implemented in this study and also location of sensors are summarized in Table 2 and Fig. 8. As it is shown in Fig. 8, a total number of 12 FBG sensors (10 on the first girder and 2 on the second girder) are employed to instrument and monitor the 4-span bridge.

Fig. 7 Experimental test conducted on the 4-span bridge using radio controlled vehicle

Table 2 Different types of damage scenarios

Global Damage Scenarios			Local Damage Scenarios	
Case 1: Fixing the first bearing	Case 2: Fixing the first two bearings	Case 3: Fixing the middle bearings	Case 4: Removing 4 bolts close to middle bearing	Case 5: Removing 8 bolts on both side of middle bearing

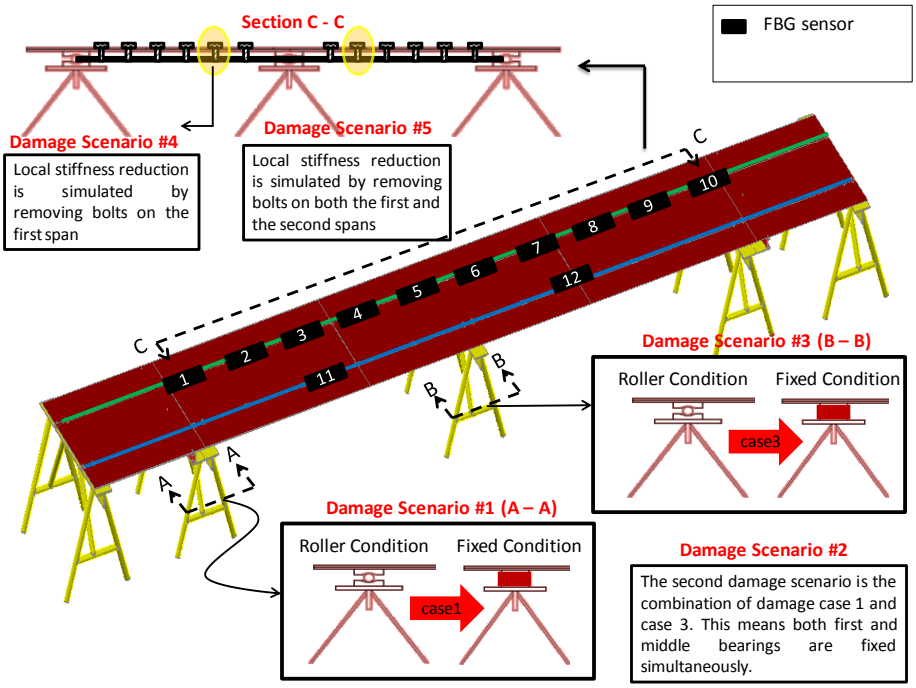

Fig. 8 Location of sensors and simulated damage (UCF 4-span Bridge)

5. Pre-processing the data

Prior to applying MPCA and MCCA algorithms to the raw data obtained from FBG sensors distributed over the bridge (and it is discussed through section 4.1), a critical issue is pre-processing of the data, which consist both low and high frequency strain responses. However high frequency part of the strain measurements is not desired in this study since the correlation between various sensors may be inversely affected by the high frequency data. As a result, high frequency data should be filtered out by using a low pass filter. In fact, the high frequency portion of the response is filtered out by transferring the response from time domain to frequency domain, and transferring the data corresponds to low frequency contents back to time domain. As it is obtained from frequency response analysis, also shown in Fig. 9, the first fundamental frequency of structure is 4.08 Hz while the second one is 7.4 Hz. Therefore, the cut off value was selected as 2 Hz. This means that portion of the response corresponds to frequency higher than 2 HZ is filtered out and the rest is shifted back to the time domain for MPCA and MCCA analysis.

6. Damage assessment

The first three damage scenarios, altering the boundary conditions, are designed for evaluating the capability of the algorithms for global damage detection while the last two damage cases are simulated to test these algorithms for local damage detection. A total of 30 data sets, 15 from

baseline condition and 15 from damage condition, were considered in this study. Each data set consisted of approximately 10000 to 13000 data points. This results in a main matrix with 360175 rows (data points or measurements) and 12 columns (number of FBG sensors or variables). Taking this information into account, the size of the moving window was chosen as 13000 x 12. The logic behind selecting the size of window as 13000 x 12 is the periodic variability in the data. In other words, the size of window is directly influenced by periodic variability of the time series. The size of window has to be selected at least as long as the largest period in the data. Therefore, in this study the size of window is selected as 13000 (data points) due to the fact that the maximum periodicity of the data is 13000 (data points).

In order to develop a confidence interval, the first 50000 points have been considered as training (baseline) phase for both MPCA and MCCA algorithms. In fact, the first 193875 points (measurements) out of 360175 points are captured from a baseline structure while only the first 50000 points are involved in developing a confidence interval. For illustration purpose, results from selective sensors (some sensor near induced damage and some sensors away from the location of damage) are presented for MPCA and MCCA. Consequently, in order to conduct a comparative study as well as to fully understand the capability of the algorithms for both global and local damage detection, two sensors close to damage location and one senor away from damage were selected for illustration purposes. The reason for this selection is that there are 12 individual FBG sensors installed on the 4-span Bridge and presenting results of MPCA and MCCA algorithms for each individual sensor is not appropriate.

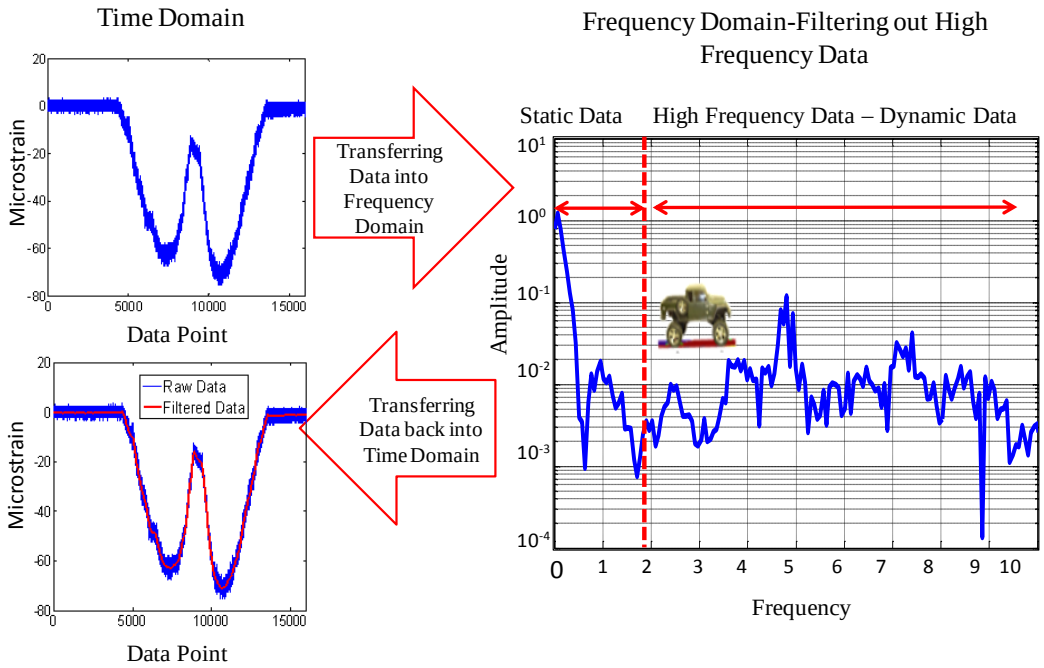

Fig. 9 Conversion of responses to frequency domain and filtering out the high frequency response

Therefore, for the first three cases, the MPCA and MCCA results corresponding to sensor 1 (close to first bearing), sensor 5 (close to middle bearing) and sensor 10 (close to third bearing) are presented. On the other hand, for case 4 (local stiffness reduction) sensors 4 and 6 (both close to damage locations) and sensor 10 (away from damage location) are selected. Correspondingly, for case 5 (severe local stiffness reduction), sensors 4 and 7, which are both located close to the location of removed bolts and sensor 10 (away from damage location) were selected as representative sensors for evaluating the efficiency of MPCA and MCCA algorithms. In the following subsections the corresponding results for both MPCA and MCCA and different scenarios will be discussed.

6.1 Global damage scenarios

6.1.1 First damage scenario (Case1: fixing the first bearing)

The main idea behind this damage case is to simulate one of the most common faults in bridge type structures, which is the change in the boundary conditions from roller condition to fixed condition. In fact, this type of change will result in redistribution of force in the structure and may cause unexpected bending moment at boundary location which can have detrimental effect on the performance of the structure. The corresponding results for MPCA and MCCA are presented in Figs. 10 and 11, respectively. Each graph, as it was mentioned formerly, is separated into two parts so called training and monitoring phase which were explained in detail through section 3.2. As it is observed from Fig. 10, MPCA precisely detected the abnormal behavior due to this damage. Dramatic change in the damage index based on the first two principal components for sensor 1 is detected while only slight change is noticed for sensor 5 (274.8 cm from the damage location) and almost no change at the location of sensor 10 (609.6 cm from the damage location).

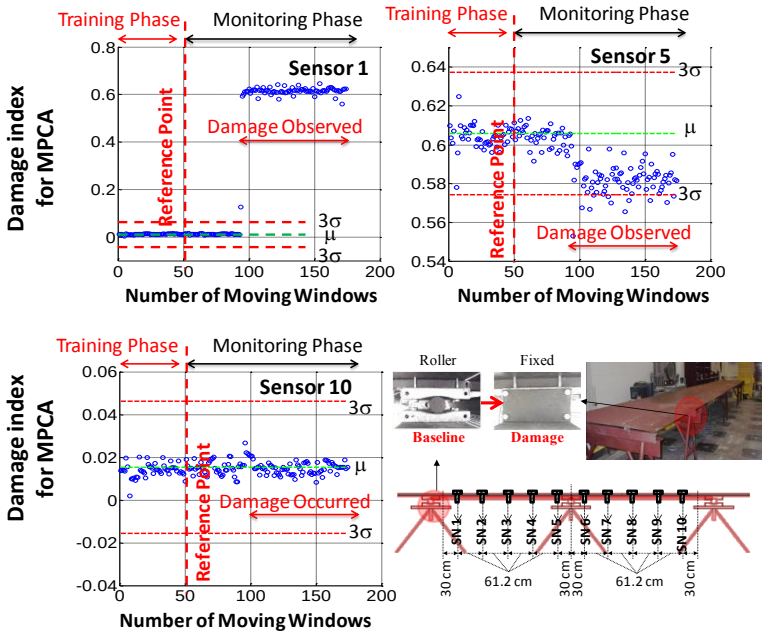

Fig. 10 MPCA results for selected sensors (Case1)

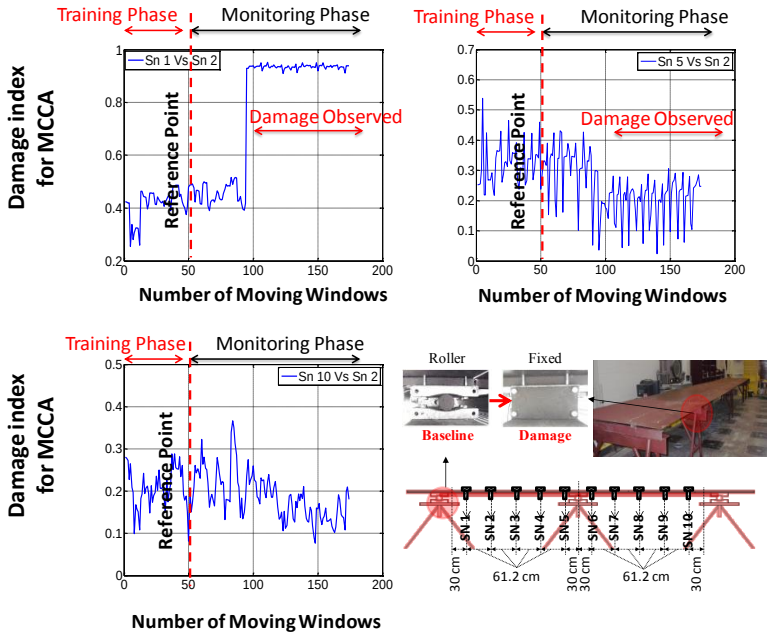

Fig. 11 MCCA results for selected sensors (Case1)

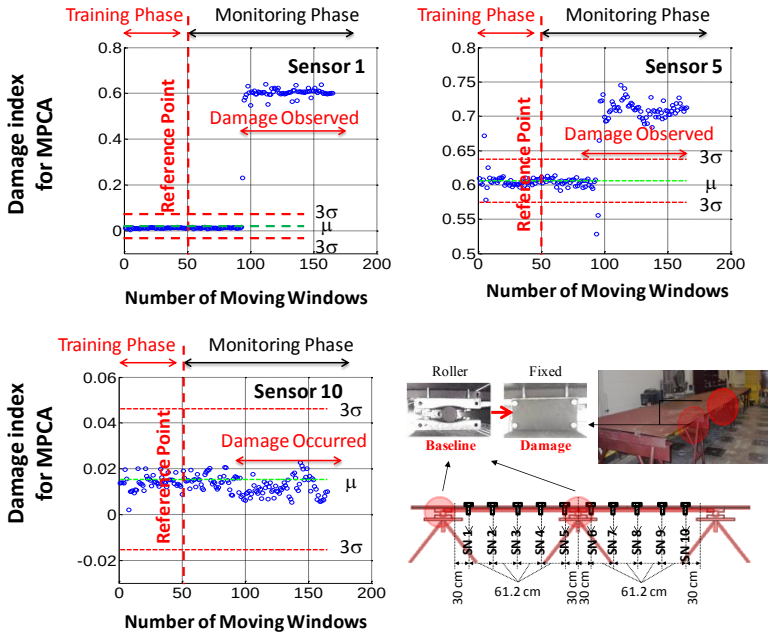

Fig. 12 MPCA results for selected sensors (Case 2)

In other words, shifting the boundary condition from roller into fixed condition caused unexpected extra moment force at the location of sensor 1 which subsequently resulted in dramatic shift in damage index value computed from this sensor. This alteration, force redistribution, is even slightly sensed over sensor 5 close to the middle bearing which is predictable based on structural analysis since it is a continuous section. In contrast, there is no abnormality detected for sensor 10, which is located 609.6 cm from the damage location. As a result, it can be mentioned that with 99.7 percent confidence that the structure around this sensor has not experienced any force redistribution issue. In the case of MCCA, Fig. 11, the correlation of sensor 1 with sensor 2, showed obvious variations after damage occurred. However, slight change over sensor 5 and no significant alteration over sensor 10 are observed. The authors realized that MCCA is slightly faster than MPCA in terms of the required time to detecting the damage. This is due to the fact that eigenvalues are only influenced when there are significant amount of data available from damage structure.

In fact, variation in damage index value due to damage was detected after conducting PCA on 98 moving windows while correlation coefficient values are affected by data from the damage of structure after performing coefficient analysis on 94 windows. Moreover, it should be also mentioned that, in terms of computational time needed for each algorithm, MCCA algorithm is superior. Computational time is also due to the fact that significantly more complicated mathematical calculations are involved in MPCA.

6.1.2 Second damage scenario (Case 2: fixing the first two bearings)

The second damage scenario was designed and implemented to simulate a situation in which a number of bearings are experiencing unintended fixing. For that reason, the middle bearing was fixed in addition to the first one. The results for this case are summarized in Figs. 12 and 13. In the second case, the sensor 1 again shows the most dramatic change similar to case 1. Additionally, in this case an abrupt jump is observed in the location of sensor 5 (close to the middle bearing). This damage is perhaps the most severe damage scenario which is simulated in this study and it can be noticed from the results. The PCA and coefficient values for both sensor 1 and 5 show obvious change after damage occurred. In fact, all the sensors located on the first span of the girder 1 experienced the same situation. For sensor 10, MPCA and MCCA are displaying slightly different results. MPCA, Fig. 12, is not able to detect any changes over the location of sensor 10 while MCCA, Fig. 13, detect some variation around that location. In fact, considering the structural configuration, some minor changes (force redistribution) would be anticipated at the location of sensor 10.

In other words, MPCA algorithm failed to detect this minor change over the last boundary condition while MCCA detects the same minor effect. Comparing the results of sensor 10 reveals the fact that MPCA may have less potential than MCCA in detecting minor change. MCCA was able to separate damage and baseline condition more clearly even at the location which experienced less damage. Even for case 1, in which the unexpected bending moment due to damage was not expected to be significant around sensor 10, MCCA was able to detect some very small variation around that location while MPCA did not express any variation at all, see Fig. 10 and Fig. 11.

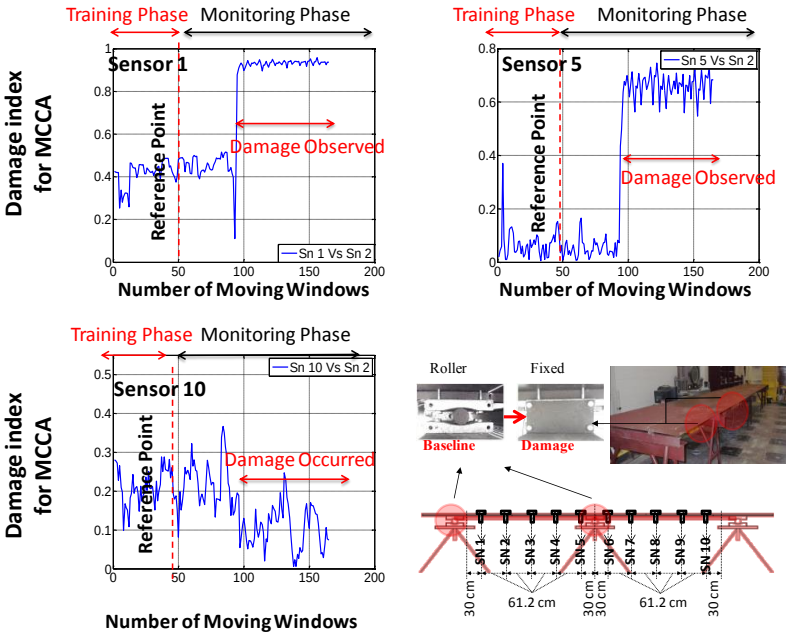

Fig. 13 MCCA results for selected sensors (Case2)

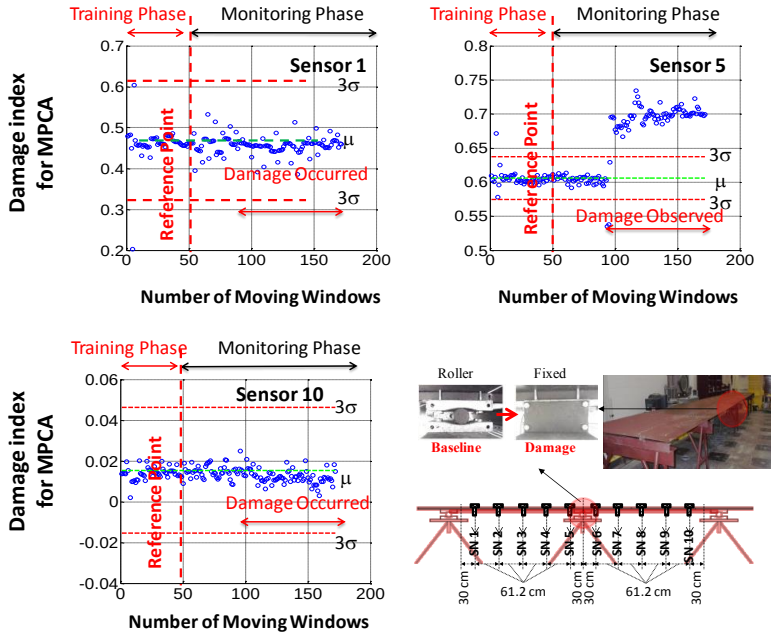

Fig. 14 MPCA results for selected sensors (Case3)

6.1.3 Third damage scenario (Case 3: fixing the middle bearings only)

MPCA and MCCA outcomes for the third case are plotted in Figs. 14 and 15, respectively. Since only the middle boundary condition is altered, only sensor 5 experienced a significant change. However, it is expected to have some minor unexpected force redistribution near the first and the last boundary. It is observed from MPCA results that only sensor 5 expresses damage while almost there is no significant variation detected around sensor 1 (located 274.8 cm from the damage location) and sensor 10 (also located 274.8 cm from the damage location). This fact was pointed out in the previous case as well. In fact, MPCA failed to detect minor change (force redistribution) occurred away from location of damage.

Instead, MCCA, Fig. 15, could detect and report the minor variation occurred around sensor 1 and 10. Correlations of sensor 1 and 10 with other sensors show some slight changes due to this case. In other words, these results also confirmed that the correlation coefficient values are more sensitive to minor damage than the Principal Component (PC) values. This case was the last global damage scenario, which was considered for this investigation. It was noticed that both MCCA and MPCA algorithms are effective enough in detecting, localizing and also revealing information about the intensity of global damage. However, MCCA outperforms MPCA in terms of detecting minor changes even far away from the location of damage. In the next section the capability of these algorithms in detecting local damage is studied.

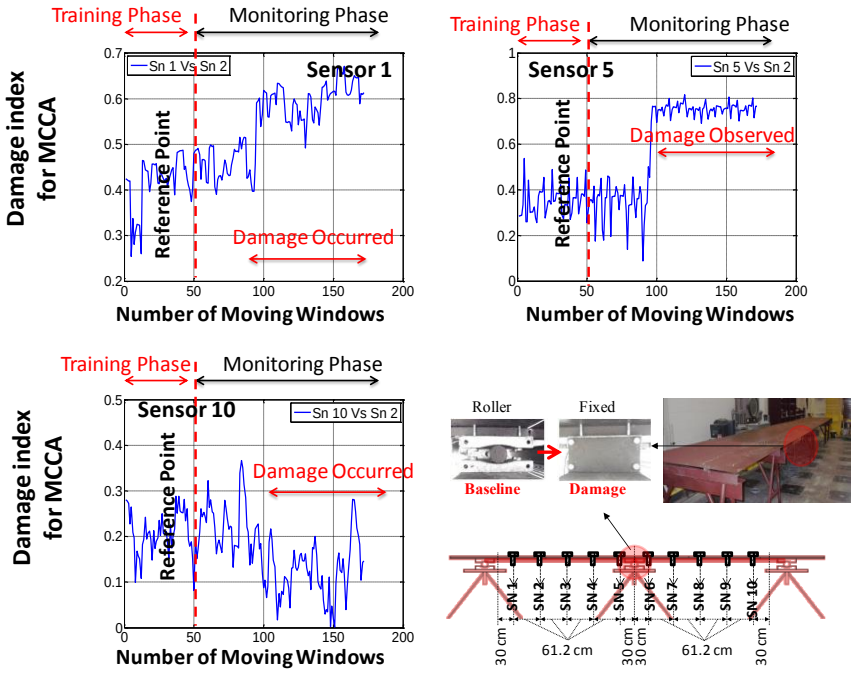

Fig. 15 MCCA results for selected sensors (Case 3)

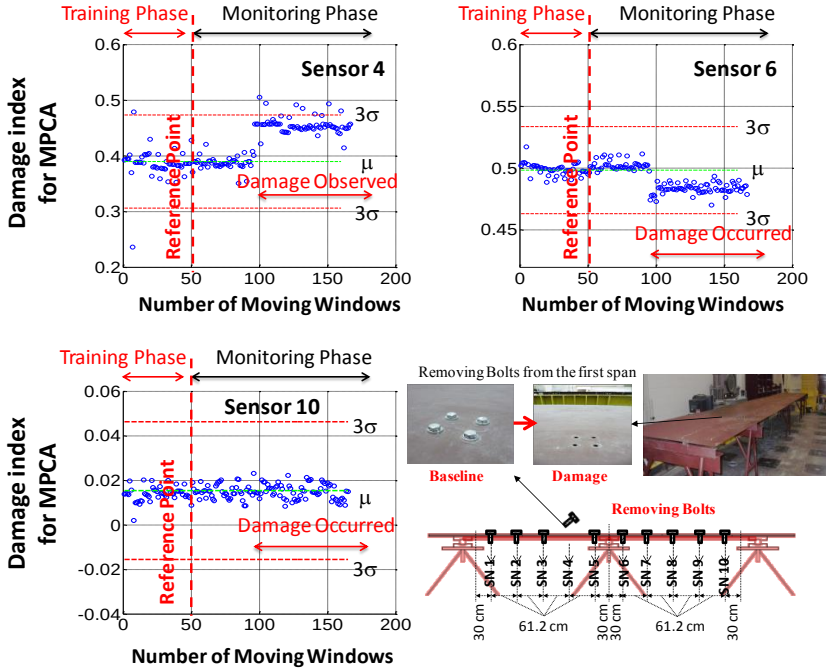

Fig. 16 MPCA results for selected sensors (Case 4)

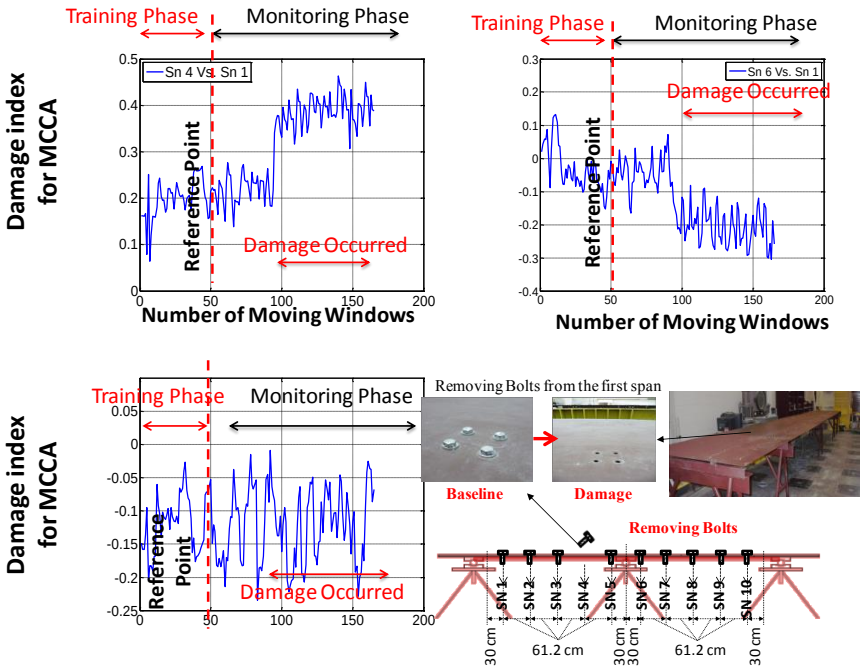

Fig. 17 MCCA results for selected sensors (Case 4)

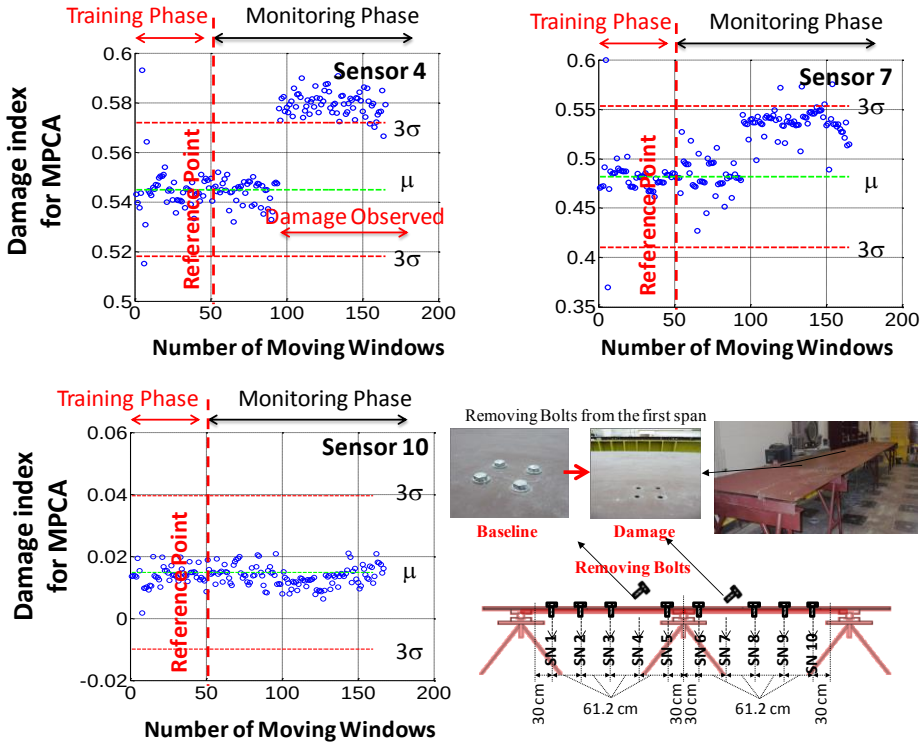

Fig. 18 MPCA results for selected sensors (Case 5)

6.2 Local damage scenarios

6.2.1 Fourth damage scenario (Case 4: removing four bolts)

The fourth scenario is a local damage, which is common in bridge type of structures. This damage scenario deals with lack of local connectivity which was simulated on the 4-span bridge by removing four bolts from the first span and close to middle bearing (91.2 cm from the middle boundary). As seen in Fig. 16, the MPCA algorithm detects significant change at the position of sensor 4, which is at the location of the removed bolts (213.6 cm from the first bearing).

In addition, changes in principal component values are noticed to some extent around sensor 6 as well but not at the location of sensor 10. Similar results are obtained by MCCA algorithm which presented in Fig. 17. Performance of MPCA and MCCA for this case is very similar except for sensor 10 in which MCCA shows more variation than MPCA. This fact was also discussed in detail through the global damage assessment section.

6.2.2 Fifth damage scenario (Case5: removing eight bolts)

To end with, the last damage scenario simulates a distributed lack of local connectivity. For this reason, another four bolts are removed from the second span which adds up to 8 removed bolts.

Principal component values corresponding to both sensor 4 (close to the four bolts removed from first span and 182.4 cm from the four bolts removed from the second span) and sensor 7

(close to 4 bolts removed from second span and 182.4 cm from the four bolts removed from the first span) were affected due to this damage. However, this value has not experienced any significant change around sensor 10. Similar observations can be made for MCCA method. The results for MPCA and MCCA are summarized in Figs. 18 and 19, respectively. The only dissimilarities which can be noticed by comparing results from MPCA and MCCA for sensor 10, is that MCCA algorithm again shows better potential in detecting minor change occurred away from the location of damage. Taking these two local induced damage scenarios into account and evaluating the MPCA and MCCA for detectibility purpose, it is revealed that these methods are efficient not only in terms of detection but also in the sense of measuring the intensity of abnormal behavior as the sensors get closer to the "damaged" area. Having considered all the damage scenarios, it is understood that the separations observed in damage indices as a result of global damage scenarios are significantly higher than the ones observed for local damage scenarios. This motivates the authors to extend the results presented in this paper to the other studies whereby the damage is not only detected but also classified using classification techniques. Future papers by the authors are expected to report their work on settingthres holds for different type of global and local damages, and subsequently classifying these damages.

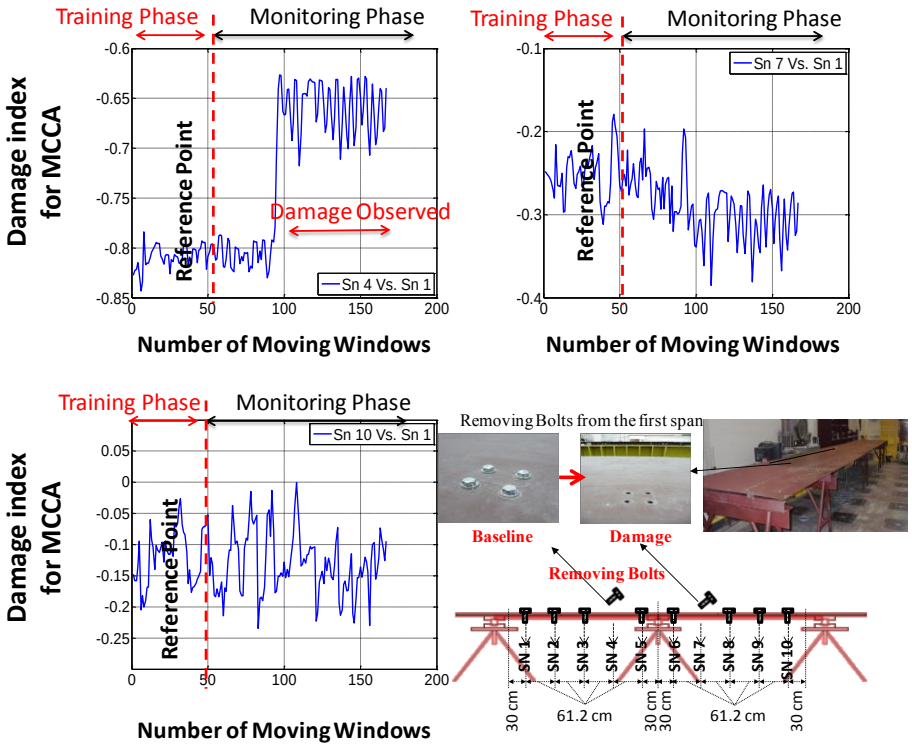

Fig. 19 MCCAresults for selected sensors (Case 5)

7. Conclusions

The damage detection ability of two advanced multivariate statistics based algorithms is investigated for long term bridge monitoring application (long term response of structure was simulated) by taking advantage of FBG sensors. MPCA and MCCA are two methods, which show promising results for real life and long term SHM. The effectiveness of these algorithms was tested using a laboratory bridge structure instrumented with fiber optic sensors. The most common and critical damage scenarios have been selected and simulated on the structure including three global and two local damage scenarios. Afterwards, the proficiencies of MPCA and MCCA are tested for each case in damage detection, localization and intensity aspects. The results conceal that these methods are very promising for long term monitoring of structures. In fact, both of these non-parametric damage detection algorithms were successful in detecting and localizing the damage under different types of simulated scenarios. However, there are some aspects in which MCCA outperforms MPCA especially for minor damage cases. MCCA has the ability to detect the damage sooner than MPCA. In addition, MCCA is superior in terms of computational time. This aspect was noticed in almost every damage scenario. As a follow up study, these algorithms will be employed and further investigated by the data collected from a unique real-life structure. It can be concluded that the correlation coefficients are more sensitive to minor variation and alteration than PC values. It is also observed that, MCCA algorithm has a better performance in detecting minor structural changes. This is due to the fact that MPCA algorithm involves more complex and time consuming procedure and calculations. This aspect may make the MCCA more desirable for real life application in which dealing with the large amounts of data is one of the main challenges.

References

Aktan, A.E., Catbas, F.N., Grimmelsman, K.A. and Tsikos, C.J. (2000), "Issues in infrastructure health monitoring for management", *J. Eng. Mech. - ASCE*, **126**(7), 711-724.

Aktan, A.E., Farhey, D.N., Brown, D.L., Dalal, V., Helmicki, A.J., Hunt, V.J. and Shelley, S.J. (1996), "Condition assessment for bridge management", *J. Infrastruct. Syst.*, **2**(3), 108-117.

Ansari, F. (2005), "Fiber optic health monitoring of civil structures using long gage and acoustic sensors", *Smart Mater. Struct.*, **14**(3), doi:10.1088/0964-1726/14/3/001.

ASCE (2013), *ASCE report cards for Americas infrastructure*, Tech. Rep. American Society of Civil Engineers, Washington, DC, USA.

Balageas, D. (2006), *Introduction to structural health monitoring*, 13-43, ISTE.

Brownjohn, J., Tjin, S.C., Tan, G.H., Tan, B.L. and Chakraboorty, S. (2004), "A structural health monitoring paradigm for civil infrastructure", *Proceedings of the 1st FIG international symposium on engineering surveys for construction works and structural engineering*.

Brownjohn, J.M.W., Zasso, A., Stephen, G.A. and Severn, R.T. (1995), "Analysis of experimental data from wind-induced response of a long span bridge", *J. Wind Eng. Ind. Aerod.*, **54**, 13-24.

Cardini, A.J. and DeWolf, J.T. (2009), "Long-term structural health monitoring of a multi-girder steel composite bridge using strain data", *Struct. Health Monit.*, **8**(1), 47-58.

Catbas, F.N., Gokce, H.B. and Gul, M. (2012), "Nonparametric analysis of structural health monitoring data for identification and localization of changes: Concept, lab, and real-life studies", *Struct. Health Monit.*, **11**(5), 613-626.

Catbas, F.N., Gul, M., Zaurin, R., Gokce, H.B., Terrell, T., Dumlupinar, T. and Maier, D. (2010), *Long term bridge maintenance monitoring demonstration on a movable bridge: A framework for structural health monitoring of movable bridges.*

Catbas, F.N., Kijewski-Correa, T. and Aktan, A.E. (2013), "Structural identification of constructed systems: Approaches, methods, and technologies for effective practice of St-Id", *American Society of Civil Engineers (ASCE) Structural Engineering Institute (SEI)*, ISBN 978-07-8441-1971 (234 pages)

Catbas, F.N. and Kijewski-Correa, T. (2013), "Structural identification of constructed systems: A collective effort toward an integrated approach that reduces barriers to adoption", *J. Struct. Eng. - ASCE*, **139**(10), 1648-1653.

Chang, F. K. (1999), *Structural health monitoring 2000*, CRC.

Enright, M.P. and Frangopol, D.M. (1999), "Condition prediction of deteriorating concrete bridges using Bayesian Aupdating", *J. Struct. Eng. – ASCE*, **125**(10), 1118-1125.

Farrar, C.R. and Worden, K. (2007), "An introduction to structural health monitoring", *Philos. T. R. Soc. A.*, **365**(1851), 303-315.

Ferdinand, P., Magne, S., Dewynter-Marty, V., Martinez, C., Rougeault, S. and Bugaud, M. (1997), Applications of Bragg grating sensors in Europe, In *Optical Fiber Sensors*, Optical Society of America.

Glisic, B. and Inaudi, D. (2008), *Fibre optic methods for structural health monitoring*, Wiley-Interscience.

Hill, K.O., Fujii, Y., Johnson, D.C. and Kawasaki, B.S. (1978), "Photosensitivity in optical fiber waveguides: Application to reflection filter fabrication", *Appl. Phys. Lett.*, **32**, 647.

Inaudi, D. (2002), *Photonic sensing technology in civil engineering applications*, Handbook of Optical Fibre Sensing Technology, Chichester.

Kwon, I.B., Baik, S.J., Im, K. and Yu, J.W. (2002), "Development of fiber optic BOTDA sensor for intrusion detection", *Sensors Actuat. A – Phys.*, **101**(1), 77-84.

Kwon, I.B., Malekzadeh, M., Ma, Q., Gokce, H., Terrell, T.K., Fedotov, A. and Catbas, F.N. (2011), *Fiber optic sensor installation for monitoring of 4 span model bridge in UCF*, Rotating Machinery, Structural Health Monitoring, Shock and Vibration, Springer New York.

Johnson, G.A., Pran, K., Wang, G., Havsgard, G.B. and Vohra, S. (1999), "Structural monitoring of a composite hull air cushion catamaran with a multi-channel fiber Bragg grating sensor system", *Proceedings of the 2nd Int. Workshop on Structural Health Monitoring*, Stanford, CA .

Lanata, F. (2005), *Damage detection algorithms for continuous static monitoring of structures (Doctoral dissertation*, PhD Thesis Italy University of Genoa DISEG).

Laory, I., Trinh, T.N. and Smith, I.F. (2011), "Evaluating two model-free data interpretation methods for measurements that are influenced by temperature", *Adv. Eng. Inform.*, **25**(3), 495-506.

Malekzadeh, M. and Catbas, F.N. (2012), "Monitoring of bridge performance by Brillouin Optical Time Domain Analysis (BOTDA) Sensig", *Proceedings of the Joint Conference of the Engineering Mechanics Institute and 11th ASCE Joint Specialty Conference on Probabilistic Mechanics and Structural Reliability (EMI/PMC 2012)*, Notre Dame, Indiana, US.

Malekzadeh, M., Gul, M. and Catbas, F.N. (2012), *Use of FBG sensors to detect damage from large amount of dynamic measurements*, In Topics on the Dynamics of Civil Structures, Springer, US.

Malekzadeh, M., Gul, M. and Catbas, F.N. (2013), "Application of multivariate statistically based algorithms for civil structures anomaly detection", *Proceedings of the 31th International Modal Analysis Conference*, Feb 11-14, Garden Grove, California, USA.

Meltz, G., Morey, W. and Glenn, W. H. (1989), "Formation of Bragg gratings in optical fibers by a transverse holographic method", *Opt. Lett.*, **14**(15), 823-825.

Morey, W.W., Meltz, G. and Glenn, W.H. (1990), "Fiber optic Bragg grating sensors", *Proceedings of the OE/FIBERS'89* , International Society for Optics and Photonics.

Mujica, L.E., Rodellar, J., Fernandez, A. and Güemes, A. (2011), "Q-statistic and T2-statistic PCA-based measures for damage assessment in structures", *Struct. Health Monit.*, **10**(5), 539-553.

Robert-Nicoud, Y., Raphael, B. and Smith, I.F. (2005), "System identification through model composition and stochastic search", *J. Comput. Civil. Eng.*, **19**(3), 239-247.

Omenzetter, P., Brownjohn, J.M.W. and Moyo, P. (2004), "Identification of unusual events in multi-channel bridge monitoring data", *Mech. Syst. Signal Pr.*, **18**(2), 409-430.

Posenato, D., Lanata, F., Inaudi, D. and Smith, I.F. (2008), "Model-free data interpretation for continuous monitoring of complex structures", *Adv. Eng. Inform.*, **22**(1), 135-144.

Puentes, R. (2008), A bridge to somewhere: Rethinking American transportation for the 21st century.
Richards, W.L., Parker, J., Ko, W.L., Piazza, A. and Chan, P. (2012), Application of fiber optic instrumentation (Validation des systemesd'instrumentation a fibresoptiques).
Sohn, H., Farrar, C.R., Hemez, F.M., Shunk, D.D., Stinemates, D.W., Nadler, B.R. and Czarnecki, J.J. (2004), *A review of structural health monitoring literature: 1996-2001* (p. 303). Los Alamos,, New Mexico: Los Alamos National Laboratory.
Todd, M.D., Johnson, G.A., Chang, C.C. and Malsawma, L. (2000), "Real-time girder deflection reconstruction using a fiber Bragg grating system", *Proceedings of the Int. Modal. Analysis, Conf. XVIII*.
Todd, M., Johnson, G., Vohra, S., Chen-Chang, C., Danver, B. and Malsawma, L. (1999), "Civil infrastructure monitoring with fiber Bragg grating sensor arrays", *Proceedings of the 2nd Int. Workshop on Structural Health Monitoring* , Stanford University, Stanford, CA, September 8-10.
Vohra, S.T., Todd, M.D., Johnson, G.A., Chang, C.C. and Danver, B.A. (1999), "Fiber Bragg grating sensor system for civil structure monitoring: applications and field tests", *Proceedings of the Society of Photo-Optical Instrumentation Engineers (SPIE) Conference Series*.
Worden, K. (1997), "Structural fault detection using a novelty measure", *J. Sound Vib.*, **201**(1), 85-101.
Worden, K. and Dulieu-Barton, J.M. (2004), "An overview of intelligent fault detection in systems and structures", *Struct. Health Monit.*, **3**(1), 85-98.
Yin, S., Ruffin, P.B. and Francis, T.S. (2008), *Fiber optic sensors* , CRC Press ILlc.
Zaurin, R. and Catbas, F.N. (2011), "Structural health monitoring using video stream, influence lines, and statistical analysis", *Struct. Health Monit.*, **10**(3), 309-332.

CY